

Article

# Effect of Glow-Discharge Plasma Treatment on Contact Angle and Micromorphology of Bamboo Green Surface

Xuehua Wang <sup>1,\*</sup> and Kenneth J. Cheng <sup>2</sup> 

<sup>1</sup> Department of Furniture and Wooden Products, College of Furnishings and Industrial Design, Nanjing Forestry University, Nanjing 210037, China

<sup>2</sup> Department of Wood Science, Forest Sciences Centre, University of British Columbia, Vancouver, BC V6T 1Z4, Canada; kyeser22@gmail.com

\* Correspondence: wangxuehua@njfu.edu.cn; Tel.: +86-025-8542-7528

Received: 24 October 2020; Accepted: 25 November 2020; Published: 30 November 2020



**Abstract:** The inner and outer surfaces of bamboo stems are usually removed prior to the manufacture of bamboo panels because the surfaces are hydrophobic and difficult to bond with glue. Hence, the recovery and utilization ratio of bamboo during processing is low. This study focused on using glow-discharge plasma to treat green bamboo surfaces to make them less hydrophobic. The effects of plasma treatment on green bamboo stems were examined using contact goniometry (wettability), non-contact confocal profilometry and scanning electron microscopy (SEM). Confocal profilometry and SEM revealed that the morphology of green bamboo surfaces varied between 3 different stems. Plasma was able to etch bamboo green surfaces, and make them rougher and more powdery. Plasma treatment was effective at converting green bamboo surfaces from hydrophobic (initial contact angle  $>110^\circ$ ) to hydrophilic (contact angle  $<20^\circ$ ). However, this effect was temporary and contact angle increased with time and recovered approximately 30% of its original value after 24 h. Based on our findings, we conclude that plasma treatment can alter parameters such as surface energy and roughness that could improve glue bonding of green bamboo, but delays between plasma treatment and further processing would need to be minimized.

**Keywords:** bamboo; bonding; surface treatment; modification; 3D topography

## 1. Introduction

As primary forest area declines, fast growing bamboo is becoming more important as a source of biomaterials especially for forest-deficient countries, such as India, China, and so on. The bamboo industry supplies earnings, food, and fibre for more than 2.2 billion people; half the world's population is involved in using and trading bamboo products. Manufactured bamboo is widely used in many fields, such as furniture, buildings, musical instruments, and so on. As a biological material, bamboo has the advantage of fast growth, low energy consumption during processing and much higher strength compared with other herbaceous plants. Some of its mechanical properties compare favourably with those of wood. For example, Yang et al. studied three species of eucalypt wood (*E. globulus* Labill, *E. nitens* (H. Deane & Maiden) Maiden, *E. regnans* F. Muell.), with Modulus of Elasticity (MOE) of 18 GPa, 11 GPa, 13 GPa, and Modulus of Rigidity (MOR) of 119 MPa, 83 MPa, 83 MPa respectively [1]. Daian et al. reported that the MOE and MOR for Australian ponderosa pine (*Pinus ponderosa* Douglas ex C. Lawson) wood were 7.7 GPa and 65.3 MPa, respectively [2], whereas the MOE of *Bambusa rigida* (Keng & Keng f.) bamboo was 12.8 GPa and MOR was 119.8 MPa [3]. Furthermore, the MOE of *Dendrocalamus farinosus* ((Keng & Keng f.) L.C.Chia & H.L.Fung) bamboo was as high as 68.7 GPa and its MOR reached 255.0 MPa [3].

Although it has many advantages, bamboo's uses and ease of mechanical processing are lower than those of wood, largely because of its hollow structure, small diameter and hard and hydrophobic outer stem surface. In order to use bamboo it is usually manufactured into composites such as bamboo Scrimber™, bamboo plywood, bamboo laminated lumber, and so on. One of the first steps in making bamboo composites is to remove its outer green surface and its inner yellow surface because these layers interfere with glue bonding. These processing steps increase the complexity of making composites from bamboo and significantly lower bamboo's recovery rate (utilization ratio). For example, the utilization ratio (from raw material to panel) of bamboo-based plywood, panel, and flooring is only 35–48%, 50%, and 20–25%, respectively [4], compared to ~60% for composites made from wood [5].

Improving surface energy and reducing hydrophobicity of bamboo stems is a potential route to improving their utilization ratio during the manufacture of composites. Numerous approaches to improving adhesion of difficult-to-glue woody materials have been tried in the past including, sanding [6], plasma treatment [7], freeze-thaw treatment [8] etc. Plasma treatment is attracting increasing attention and it has been shown to be effective at improving wood's bonding ability [9,10], but improvements are affected by species [11,12], growth direction [13], time [14], media [15], etc. Plasma treatment of bamboo has also been examined, but the research has mainly focused on treating bamboo fibers [16], bamboo powder [17,18], bamboo slivers [19], etc. By contrast the effects of plasma treatment on the properties of raw bamboo to support industrial applications of bamboo has received less attention [20].

In order to get further information about how plasma affects raw bamboo surfaces, bamboo's green side was plasma treated, and changes of contact angle, micro-roughness, and microstructure before and after plasma were examined. We anticipate that our findings could give some data for improving bamboo's surface bonding properties, adhesion, and provide useful advice for the utilization of whole bamboo.

## 2. Materials and Methods

### 2.1. Materials

Three (3) bamboo stems for three typical bamboo surface conditions, including normal, smooth and rough surfaces, were stored in a conditioning room at  $20 \pm 1$  °C and  $65 \pm 5\%$  r.h. in the Forest Science Center of UBC. The basic densities of the bamboo blocks were  $0.48 \text{ g/cm}^3$ ,  $0.55 \text{ g/cm}^3$ ,  $0.61 \text{ g/cm}^3$ , culm wall thicknesses were 5.45 mm, 7.11 mm, 5.25 mm, and moisture contents were 8.0%, 8.2%, 7.9% for bamboo stems numbered 1, 2, 3, respectively (Figure 1a). Stems were cut from the third internode from bottom (Figure 1b). Eight (8) pieces were prepared for each stem to ensure adequate replication. Small blocks with size of 5 mm (longitudinal) by 5 mm (tangential) by actual thickness were cut from bamboo sections. Compressed air was used to clean the bamboo blocks, especially the green bamboo surfaces.

### 2.2. Methods

#### 2.2.1. Plasma Treatment

A glow-discharge water vapor plasma reactor [7] was used to treat the bamboo specimens. The plasma was produced under vacuum of  $19.99 \pm 1.33$  Pa. Green bamboo surfaces were treated at 150 W for 5 min, while the control set for each stem was treated for 5 min at the same pressure without plasma.

#### 2.2.2. Contact Angle Test

Contact angles of water droplet on bamboo surfaces were obtained to determine the surface wettability and energy change resulting from plasma treatment. A KVS CAM 101 instrument (KSV Instrument Ltd., Helsinki, Finland) was used to measure the static contact angle of water

droplets on green bamboo surfaces. Images were captured once the water droplet formed and before it left the syringe needle. The filming frequency was every 16 milliseconds, with one shot lasting for 120 frames and then every second shot lasting for 20 frames. Images were captured the moment the water droplet touched the green bamboo surface and were used to calculate contact angle. Contact angles were calculated by baseline adjustment and curve fitting of the captured drop profile to the theoretical shape predicted by the Young-Laplace equation using instrument software (CAM 200, KSV Instrument 2007, Helsinki, Finland). Left and right angles were averaged to obtain a mean contact angle for each test.



**Figure 1.** Bamboo specimens: (a) bamboo blocks, (b) bamboo specimen preparation.

### 2.2.3. 3D Topography and Height Parameters

A white-light non-contact confocal profilometer (Altisurf 500 ®, ALTIMET, Marin, France) was used to measure the topography of samples before and after plasma treatment. To ensure the same area  $0.5 \times 0.5 \text{ mm}^2$  of interest (radial or tangential) was scanned before and after plasma treatment, a “L” shape wooden frame was placed on the x-y stage of the confocal profilometer. This frame ensured that bamboo specimens maintained the same position on the x-y stage during scanning. The following measurement parameters were used: spacing between measurement point  $0.5 \times 0.5 \text{ }\mu\text{m}$ ; resolution =  $1001 \times 1001$ ; scan speed =  $100 \text{ }\mu\text{m/second}$  and measurement range in the z-direction varied from  $10 \text{ nm}$  to  $300 \text{ }\mu\text{m}$ . The software PaperMap (v. 3.2.0, ALTIMET, Marin, France) was used to produce high-resolution topographic images of green bamboo surfaces. Roughness parameters  $S_q$ ,  $S_{sk}$ ,  $S_{ku}$ ,  $S_p$ ,  $S_v$ ,  $S_z$ ,  $S_a$  according to ISO 25178 were also obtained from PaperMap (v. 3.2.0) and were used to assess the effect of plasma treatment on roughness of green bamboo surfaces.

$S_q$  (root mean square value of the ordinate values within a definition area (A))-root mean square value of the ordinate values within a definition area (A).

$$S_q = \sqrt{\frac{1}{A} \int \int_A z^2(xy) dx dy} \quad (1)$$

$S_{sk}$  (skewness of the scale-limited surface)—quotient of the mean cube value of the ordinate values and the cube of  $S_q$  within a definition area (A).

$$S_{sk} = \frac{1}{S_q^3} \left[ \frac{1}{A} \int \int_A z^3(xy) dx dy \right] \quad (2)$$

$S_{ku}$  (kurtosis of the scale-limited surface)—quotient of the mean quartic value of the ordinate values and the fourth power of  $S_q$  within a definition area (A).

$$S_{ku} = \frac{1}{S_q^4} \left[ \frac{1}{A} \int \int_A z^4(xy) dx dy \right] \quad (3)$$

$S_p$  (maximum peak height of the scale limited surface)—largest peak height value within a definition area.

$S_v$  (maximum pit height of the scale limited surface)—minus the smallest pit height value within a definition area.

$S_z$  (maximum height of the scale limited surface)—sum of the maximum peak height value and the maximum pit height value within a definition area.

$S_a$  (arithmetic mean of the scale limited surface)—arithmetic mean of the absolute of the ordinate values within a definition area ( $A$ )

$$S_a = \frac{1}{A} \int \int |z(xy)| dx dy \quad (4)$$

#### 2.2.4. Scanning Electron Microscopy

The effects of plasma treatment on green bamboo surfaces was observed by SEM. The plasma modified and unmodified bamboo specimens were attached to aluminum mounting stubs using double-sided adhesive tape and dried [21]. They were then coated with gold using a sputter coater (Nanotech SEMPRep II, Nanotechnology Ltd., Sandy, UK) and examined using a field emission scanning electron microscope (Hitachi S-4700, FESEM, Hitachi High-Tech Corporation, Tokyo, Japan). The accelerating voltage was 5 kV.

### 3. Results and Discussion

#### 3.1. Contact Angle

Contact angle is an important parameter for evaluating surface energy (solid surface wettability to liquid), which affects surface finishing, and adhesive bonding [7]. When contact angle  $\theta > 90^\circ$ , the solid is defined as hydrophobic and when  $\theta < 90^\circ$  the solid is defined as hydrophilic.

Figure 2 shows contact angle change of green bamboo surface after glow-discharge plasma treatment. Green bamboo surfaces were converted from hydrophobic to hydrophilic after plasma treatment. Their initial contact angle dropped from  $115^\circ$  to  $14^\circ$  (Figure 2a). This contact angle decrease is similar to that of bamboo treated using a low pressure cold radio frequency (RF) discharge plasma (contact angle on bamboo green surface changed from  $109^\circ$  to  $19^\circ$ , as evaluated using 2D resin [20]). However, the change is larger than that of bamboo treated with a cold oxygen plasma (contact angle decreased from  $104^\circ$  to  $52^\circ$ , as evaluated using phenol formaldehyde resin [22]). As time elapsed, contact angle recovered, especially during the first 24 h. Contact angle of stem 2 after 24 h of plasma treated recovered 84% of its original value (Figure 2b).

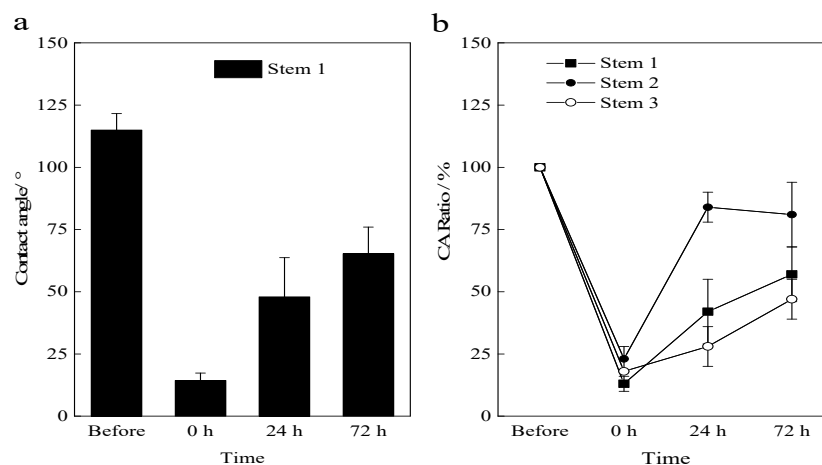


**Figure 2.** Contact angle: (a) contact angle changes of stem 1 during aging, (b) contact angle ratio of plasma treated specimens compared to untreated control during aging.

Our finding that effect of plasma treatment on wettability is not permanent, and contact angle recovers as time elapses has been observed with other materials [23]. For example, wettability of European beech (*Fagus sylvatica* L.) after atmospheric plasma treatment decreased significantly in the following two days [24]. In the case of polyethylene (PE), contact angle decreased from  $97^\circ$  to  $0^\circ$  after treatment with a radio frequency capacitively coupled oxygen plasma, but the PE became superhydrophobic 24 h later, with contact angle increasing to  $150^\circ$  [25]. This aging effect is thought to be caused by both ‘thermodynamically driven reorientation of induced polar functional groups into the bulk of the material to reduce the surface energy and the diffusion of the polar chemical groups in the polymer matrix’ [26], and is ‘influenced by parameters such as substances, degree of crystallinity of treated material, plasma gas species, storage conditions’ [27,28], or even different stems (in this research, stem 2 recovered more than 80% of its initial contact after 24 h, while recovery by stem 1 and stem 3 was less than 40% (Figure 2b)). Hence, because of the effects of aging on contact angle of plasma treated green bamboo surfaces, any subsequent processing steps such as coating or bonding, should be done immediately after plasma treatment.

### 3.2. 3D Topography and Height Parameters

As a non-contact topography measurement technique, confocal profilometry is especially suitable for measuring the roughness of irregular, curved surfaces, such as those present in the green bamboo specimens treated here. The 3D topography of green bamboo surfaces before and after plasma treatment are shown below in Figure 3.

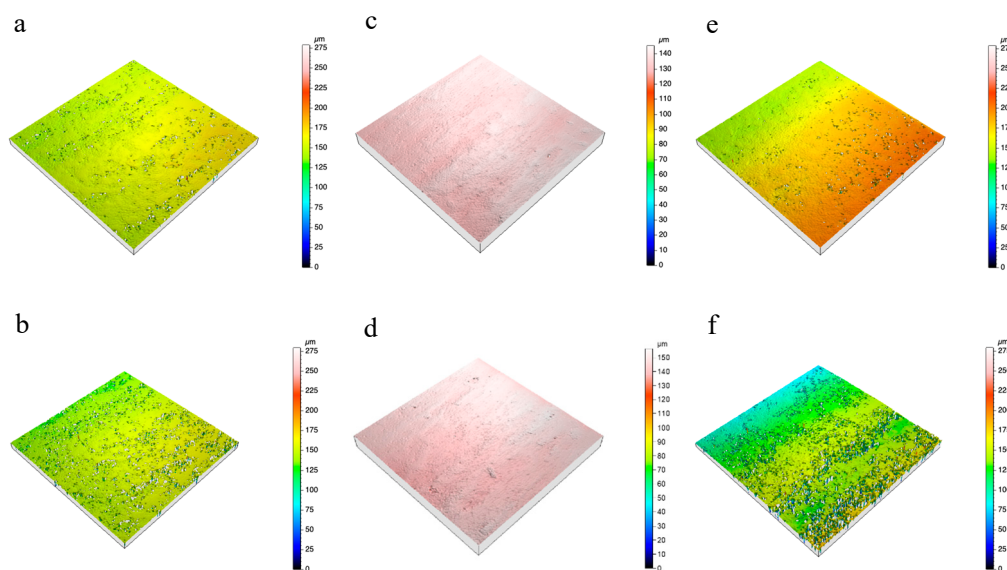


**Figure 3.** 3D topographical images obtained by confocal profilometry for (a) stem 1, before plasma treatment, (b) stem 1, after plasma treatment, (c) stem 2, before plasma treatment, (d) stem 2, after plasma treatment, (e) stem 3, before plasma treatment, and (f) stem 3, after plasma treatment.

From Figure 3, it can be seen that the topography of the green bamboo surfaces before and after plasma treatment differed between the three stems. The color-coded images in Figure 3 show heights of green bamboo surfaces. The different color blocks in stem 1 and stem 3 were mainly caused by the curvature of bamboo surface resulting from their smaller diameters. The dark spots in images are produced by voids in the surface of the green bamboo specimens. Compared with obvious scattered holes on the surfaces of stem 1 and stem 3, holes on stem 2 are less visible. Holes numbers in stem 1 and stem 3 increased after plasma treatment while there was little change in the number of holes in stem 2. This finding suggests a strong between-sample, effect on plasma etching of green bamboo surfaces.

Height parameters from confocal profilometry were used to calculate surface roughness, which directly influences surface bonding strength, coating quality, and so on. Table 1 lists the different roughness parameters matched with stems in Figure 3.

**Table 1.** Height parameters of green bamboo stems before and after plasma treatment.

Parameters	Stem 1		Stem 2		Stem 3	
	Before	After	Before	After	Before	After
$S_a/\mu\text{m}$	6.48	7.90	2.10	3.03	16.1	20.1
$S_q/\mu\text{m}$	10.0	14.0	2.55	3.69	19.7	27.2
$S_{sk}$	-6.07	-6.08	-0.883	-2.32	-1.22	-1.68
$S_{ku}$	90.7	59.8	33.4	85.4	9.69	7.62
$S_p/\mu\text{m}$	125	134	7.85	9.23	108	155
$S_v/\mu\text{m}$	155	146	138	147	170	125
$S_z/\mu\text{m}$	279	280	146	156	279	280

Note: all above parameters are defined according to international standard ISO 25178-2-2012.

In accord with 3D topographical images in Figure 3, glow-discharge water vapor plasma treatment roughened and increased  $S_a$  for all three stems, (Table 1). Plasma can etch materials although the rate of etching varies between materials and in polymer blends [29,30]. The testing plane after plasma treatment might have become lower in stem 1 and stem 3 as  $S_p$  increased for these specimens while it remained largely unchanged for stem 2 ( $S_p$  changed little) (Table 1). According to the colour-coded topographic maps of the 3 stem specimens in Figure 3, height changes were mainly less than 50  $\mu\text{m}$  including scattered peaks and troughs. However, the parameter  $S_z$ , sum of the maximum peak and pit height, was close to full measurement range of 300  $\mu\text{m}$  both before and after plasma treatment (Figure 3, Table 1). This discrepancy may be due to the presence in the green bamboo specimens of narrow and deep troughs rather than peaks, as  $S_{sk}$  values were negative, far lower than  $-1$  [31],  $S_{ku}$  values were all much larger than 3, which indicates a concentrated distribution of needle valleys [32].

From  $S_a$  results it appears as though stems with lower initial  $S_a$  roughened less as a result of plasma treatment. One reason for this phenomenon might be reduced surface area on smoother surfaces for the plasma to etch the green bamboo during treatment [33–35]. Changes in  $S_p$ ,  $S_v$  and  $S_a$  after plasma treatment were greatest in stem 3, and smallest in stem 2, indicating that the surface of stem 3 was etched more easily by plasma than that of than stem 2. This finding suggests a strong effect of stem type on plasma etching of green bamboo stems.

### 3.3. Scanning Electron Microscopy

Characterization of the plasma etching of stems 1, 2, and 3 was done with SEM, which has higher magnification and better resolution of green bamboo surfaces than confocal profilometry. It must be pointed out, however, that images depend not only on the stems, but also on the place of imaging at the surface. The surface morphologies showed significant differences between the 3 stems.

In stem 1, cryptopores with oval shapes surrounded by tiny protuberance were visible both before and after plasma treatment. Green bamboo surfaces were covered by tiny protuberances (Figure 4a–d). In comparison to stem 1, stems 2 and 3 showed a smoother surface covered by platelets (Figure 4e,f) or particles (Figure 4i,j) before plasma treatment. It was difficult to see any cells at these surfaces (Figure 4e,f), which may be due to high levels of silicon,  $\text{SiO}_2 \cdot n\text{H}_2\text{O}$  or silicon compounds in green epidermis layer of the bamboo [36,37]. Platelets or particles in the epidermis layers were removed (etched) by plasma, and micro-convexes on stem 2 and cryptopores on stem 3 bamboo green surface became apparent (Figure 4g,k). Micron sized powder particles were also common (Figure 4h,l).

SEM images of stem 2 and stem 3 show smooth surfaces before plasma treatment while globular protuberances appeared after plasma treatment (Figure 4e,g,i,k) indicating etching of the surface of green bamboo by plasma. Etching effects on substance morphology is a widely reported outcome of plasma treatment, such as wood treated by cold atmospheric pressure plasma [14], hot-oil modified

wood treated with water-vapour plasma [38], polyethylene terephthalate (PET) film treated by radio frequency Ar plasma [39] and so on. Changes caused by plasma treatment of green bamboo such as roughening and appearance of globular protuberances (Table 1), could have increased surface water permeability [40], thereby contributing to decreases in contact angle (surface energy increases) [41] (Figure 2). Such plasma-induced changes could make the surface of green bamboo more bondable [42] but further research is needed to confirm this suggestion.

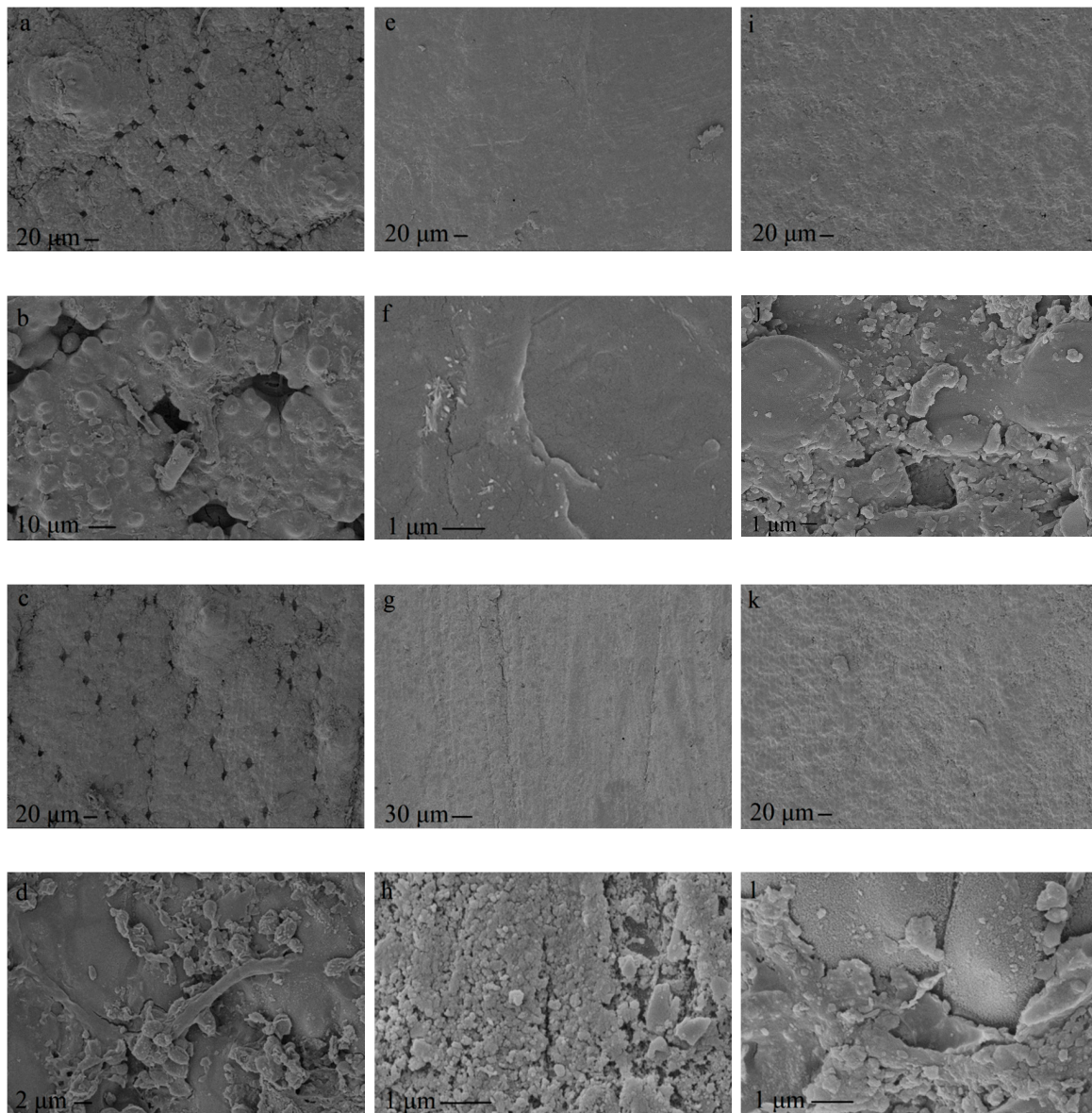


**Figure 4.** Scanning electron microscopy images of green bamboo surfaces of stem 1 untreated (a,b) & treated (c,d), stem 2 untreated (e,f) & treated (g,h), stem 3 untreated (i,j) & treated (k,l) by plasma.

#### 4. Conclusions

The effects of glow-discharge plasma on green bamboo surfaces from three different stems was examined using contact goniometry (wettability), non-contact confocal profilometry and scanning electron microscopy. Bamboo had a hydrophobic green surface with an original contact angle greater than  $110^\circ$ . Plasma treatment had the temporary effect of making green bamboo surfaces hydrophilic (contact angle below  $20^\circ$ ). However, with aging, contact angle recovered by more than 30% after 24 h and 50% after 72 h. Green bamboo surface morphology varied between stems and surfaces could

be very smooth with cells obscured by silicon compounds. Plasma treatment etched green bamboo surfaces resulting in roughness increases and changes in surface morphology including creation of a powdery layer. These surface changes and increases in specific surface area may explain in part why contact angle decreased after plasma treatment. Results here indicate that glow-discharge plasma treatment exerts a temporary effect on surface wettability of green bamboo and a more permanent effect on surface morphology. Based on our findings, we conclude that delays between plasma treatment and any processing of bamboo that requires hydrophilic surfaces such as gluing need to be minimized.

**Author Contributions:** Formal analysis and experimental operation, K.J.C. and X.W.; data curation, writing—original draft, review, and editing, X.W. All authors have read and agreed to the published version of the manuscript.

**Funding:** This research was funded by Natural Science Foundation of China, grant number 31800471. Kenneth J. Cheng was supported, in part, by funding from NSERC (Collaborative Research and Development Grant CRDPJ 485007-15).

**Acknowledgments:** We thank Philip D. Evans from Department of Wood Science, University of British Columbia for hosting Xuehua Wang's visit to UBC Faculty of Forestry and for his in-kind support of our research; Lukie H. Leung, Joseph D.W. Kim, Mohammad Sadegh Mazloomi from Department of Wood Science, University of British Columbia for assistance with plasma treatment, confocal profilometry, and contact goniometry.

**Conflicts of Interest:** The funders had no role in the design of this study; in the collection, analyses, or interpretation of data; in the writing of the manuscript, or in the decision to publish the results.

## References

1. Yang, J.L.; Evans, R. Prediction of MOE of eucalypt wood from microfibril angle and density. *Holz Als Roh-Und Werkst.* **2003**, *61*, 449–452. [\[CrossRef\]](#)
2. Daian, M.; Bucur, V.; Ozarska, B.; Daian, G. Static strength characteristics (MOR and MOE) of Australian *Pinus ponderosa* wood from plantation: A comparison of green, dry and re-wet specimens: A technical note. *J. Indian Acad. Wood Sci.* **2012**, *9*, 140–142. [\[CrossRef\]](#)
3. Yang, X.; Liu, X.; Yang, S.; Li, X.; Shang, L.; Shan, H. Comparison of Physical-Mechanical Properties of Five Sympodial Bamboo Species. *J. Northeast For. Univ.* **2013**, *41*, 91–97.
4. Zhang, H.; Liu, J.; Wang, Z.; Lu, X. Mechanical and thermal properties of small diameter original bamboo reinforced extruded particle board. *Mater. Lett.* **2013**, *100*, 204–206. [\[CrossRef\]](#)
5. Chen, Z.-L.; Fu, F.; Ye, K.-L. Present condition of wood resources utilization in China and technical measures of wood recycle. *China Wood-Based Panels* **2007**, *5*, 17–19.
6. Belfas, J.; Groves, K.W.; Evans, P.D. Bonding surface-modified Karri and Jarrah with resorcinol formaldehyde. *Holz Als Roh-Und Werkst.* **1993**, *51*, 253–259. [\[CrossRef\]](#)
7. Haase, J.G.; Leung, L.H.; Evans, P.D. Plasma pre-treatments to improve the weather resistance of polyurethane coatings on black spruce wood. *Coatings* **2019**, *9*, 8. [\[CrossRef\]](#)
8. Chen, T. Study on The Technology of Freeze-Thaw Cycles Treated on Bamboo Based Container Floor. Master's Thesis, Fujian Agriculture and Forestry University, Fuzhou, China, 2016.
9. Aydin, I.; Demirkir, C. Activation of Spruce Wood Surfaces by Plasma Treatment after Long Terms of Natural Surface Inactivation. *Plasma Chem. Plasma Process.* **2010**, *30*, 697–706. [\[CrossRef\]](#)
10. Avramidis, G.; Miltz, H.; Avar, I.; Viöl, W.; Wolkenhauer, A. Improved absorption characteristics of thermally modified beech veneer produced by plasma treatment. *Eur. J. Wood Prod.* **2012**, *70*, 545–549. [\[CrossRef\]](#)
11. Odrášková, M.; Zahoranová, A.; Tiňo, R.; Černák, M. Plasma Activation of Wood Surface by Diffuse Coplanar Surface Barrier Discharge. *Plasma Chem. Plasma Process.* **2008**, *28*, 203–211. [\[CrossRef\]](#)
12. Lux, C.; Szalay, Z.; Beikircher, W.; Kováčik, D.; Pulker, H.K. Investigation of the plasma effects on wood after activation by diffuse coplanar surface barrier discharge. *Eur. J. Wood Prod.* **2013**, *71*, 539–549. [\[CrossRef\]](#)
13. Rehn, P.; Viöl, W. Dielectric barrier discharge treatments at atmospheric pressure for wood surface modification. *Holz Als Roh-Und Werkst.* **2003**, *61*, 145–150. [\[CrossRef\]](#)
14. Galmiz, O.; Talviste, R.; Panáček, R.; Kováčik, D. Cold atmospheric pressure plasma facilitated nano-structuring of thermally modified wood. *Wood Sci. Technol.* **2019**, *53*, 1339–1352. [\[CrossRef\]](#)
15. Temiz, A.; Akbas, S.; Aydin, I.; Demirkir, C. The effect of plasma treatment on mechanical properties, surface roughness and durability of plywood treated with copper-based wood preservatives. *Wood Sci. Technol.* **2016**, *50*, 179–191. [\[CrossRef\]](#)



16. Gorjanc, M.; Savić, A.; Topalić-Trivunović, L.; Mozetič, M.; Vesel, A.; Grujić, D. Dyeing of plasma treated cotton and bamboo rayon with Fallopia japonica extract. *Cellulose* **2016**, *23*, 2221–2228. [[CrossRef](#)]
17. Liang, W.; Zhang, G.; Xu, J.; Ma, C.; Yang, W.; Li, R. Aging of Bamboo Flour / PETG Composite by Cold Plasma. *J. Northeast For. Univ.* **2014**, *42*, 119–122.
18. Zhang, G.Z.; Liang, W.C.; Xu, J.F.; Ma, C.C.; Yang, W.B. Research on pure PETG and PETG /bamboo flour composite surface with plasma pretreatment. *J. Fujian Coll. For.* **2014**, *34*, 176–183.
19. Bao, L.X.; Rao, J.P.; Lan, C.R.; Lin, Q.J.; Yang, W.B. Optimization of the plasma treatment of bamboo and its application in reconstituted bamboo lumber. *J. Fujian Agric. For. Univ. (Nat. Sci. Ed.)* **2014**, *43*, 199–203.
20. Li, B.; Li, J.X.; Zhou, X.J.; Du, G.B. Effect of Low Pressure RF Discharge Cold Plasma Treatment on Improving Surface Coating Properties of Bamboo Culms. *J. Southwest For. Univ. (Nat. Sci.)* **2019**, *39*, 135–141.
21. Heady, R.D.; Banks, J.G.; Evans, P.D. Wood anatomy of Wollemi pine (*Wollemia nobilis*, Araucariaceae). *IAWA J.* **2002**, *23*, 339–357. [[CrossRef](#)]
22. Wu, Q.R.; Guan, X.; Lin, J.G.; Li, Q.Y.; Qi, W.Y. Effect of Cold Plasma Treatment on the Surface Wettability of Bamboo. *J. Southwest For. Univ. (Nat. Sci.)* **2017**, *37*, 188–193.
23. Jelil, R.A. A review of low-temperature plasma treatment of textile materials. *J. Mater. Sci.* **2015**, *50*, 5913–5943. [[CrossRef](#)]
24. Altgen, D.; Altgen, M.; Kyyrö, S.; Rautkari, L.; Mai, C. Time-dependent wettability changes on plasma-treated surfaces of unmodified and thermally modified European beech wood. *Eur. J. Wood Prod.* **2020**, *78*, 417–420. [[CrossRef](#)]
25. Li, S. Study on Aging Behavior of Polymer Surfaces Modified by Radio Frequency Capacitively Coupled Oxygen Plasma. Master's Thesis, Dalian University of Technology, Dalian, China, 2012.
26. Yun, Y.I.; Kim, K.S.; Uhm, S.J.; Khatua, B.B.; Cho, K.; Kim, J.K.; Park, C.E. Aging behavior of oxygen plasma-treated polypropylene with different crystallinities. *J. Adhes. Sci. Technol.* **2004**, *18*, 1279–1291. [[CrossRef](#)]
27. Della Volpe, C.; Fambri, L.; Fenner, R.; Migliaresi, C.; Pegoretti, A. Air-plasma treated polyethylene fibres: Effect of time and temperature ageing on fiber surface properties and on fiber-matrix adhesion. *J. Mater. Sci.* **1994**, *29*, 3919–3925. [[CrossRef](#)]
28. Yasuda, H.; Charlson, E.J.; Charlson, E.M.; Yasuda, T.; Miyama, M.; Okuno, T. Dynamics of surface property change in response to changes in environmental conditions. *Langmuir* **1991**, *7*, 2394–2400. [[CrossRef](#)]
29. Sapiuha, S.; Wrobel, A.M.; Wertheimer, M.R. Plasma-assisted etching of paper. *Plasma Chem. Plasma Process.* **1988**, *8*, 331–346. [[CrossRef](#)]
30. Amirov, I.I.; Izyumov, M.O.; Morozov, O.V. Etching of Silicon and Silicon Dioxide in Dense Low-Pressure Inductively Coupled Radiofrequency Discharge Fluorocarbon Plasmas. *High Energy Chem.* **2003**, *37*, 328–332. [[CrossRef](#)]
31. Krolczyk, G.M.; Krolczyk, J.B.; Maruda, R.W.; Legutko, S.; Tomaszewski, M. Metrological changes in surface morphology of high-strength steels in manufacturing processes. *Measurement* **2016**, *88*, 176–185. [[CrossRef](#)]
32. Da Costa Castanhera, I.; Diniz, A.E.; Button, S.T. Effects of tool path strategies and thermochemical treatments on the surface roughness of hardened punches for hot stamping. *J. Braz. Soc. Mech. Sci. Eng.* **2020**, *42*, 214. [[CrossRef](#)]
33. Xie, Y.J.; Zhang, X.Y.; Wu, Z.R.; Chen, Y.Y. The Preparation of Modified Basalt Fiber and its Utilization on Microorganism Carrier Media. *Synth. Fiber China* **2019**, *48*, 19–22.
34. Fujiwara, Y.; Fujii, Y.; Sawada, Y.; Okumura, S. Assessment of wood surface roughness: Comparison of tactile roughness and three-dimensional parameters derived using a robust Gaussian regression filter. *J. Wood Sci.* **2004**, *50*, 35–40. [[CrossRef](#)]
35. Söğütü, C.; Nzokou, P.; Koc, I.; Tutgun, R.; Döngel, N. The effects of surface roughness on varnish adhesion strength of wood materials. *J. Coat. Technol. Res.* **2016**, *13*, 863–870. [[CrossRef](#)]
36. Qiu, Y.; Lin, L.; Zheng, Z. Study on the cuticle of bamboo stem by means of SEM-EDAX. *Trans. China Pulp Pap.* **2002**, *17*, 1–5.
37. Li, S.H.; Liu, Q.; Zhou, B.L.; de Groot, K. Calcium phosphate formation induced on silica in bamboo. *J. Mater. Sci. Mater. Med.* **1997**, *8*, 427–433. [[CrossRef](#)]
38. Jamali, A.; Evans, P.D. Plasma treatment reduced the discoloration of an acrylic coating on hot-oil modified wood exposed to natural weathering. *Coatings* **2020**, *10*, 248. [[CrossRef](#)]
39. Xie, L.; Dai, Q.; He, R.; Zhang, X. Hydrophilicity and Surface Structure of PET Films Modified by Radio Frequency Ar Plasma. *China Plast.* **2012**, *26*, 84–88.

40. Prakash, C.; Ramakrishnan, G.; Chinnadurai, S.; Vignesh, S.; Senthilkumar, M. Effect of Plasma Treatment on Air and Water-Vapor Permeability of Bamboo Knitted Fabric. *Int. J.* **2013**, *34*, 2173–2182. [[CrossRef](#)]
41. Damayanti, N.P. Preparation of superhydrophobic PET fabric from Al<sub>2</sub>O<sub>3</sub>–SiO<sub>2</sub> hybrid: Geometrical approach to create high contact angle surface from low contact angle materials. *J. Sol-Gel Sci. Technol.* **2010**, *56*, 47–52. [[CrossRef](#)]
42. Bilaniuk, M.; Howe, J.M. Wetting, Bonding and Interfacial Energy of Nanocrystalline Metal Particles on Crystalline DCH Polymer and Amorphous Carbon Substrates. *Interface Sci.* **1998**, *6*, 319–345. [[CrossRef](#)]

**Publisher’s Note:** MDPI stays neutral with regard to jurisdictional claims in published maps and institutional affiliations.



© 2020 by the authors. Licensee MDPI, Basel, Switzerland. This article is an open access article distributed under the terms and conditions of the Creative Commons Attribution (CC BY) license (<http://creativecommons.org/licenses/by/4.0/>).